Colloids and Surfaces A: Physicochem. Eng. Aspects 341 (2009) 46–52

Contents lists available at ScienceDirect

Colloids and Surfaces A: Physicochemical and Engineering Aspects

journal homepage: www.elsevier.com/locate/colsurfa

Synthesis and characterization of Fe(III)-montmorillonites for phosphate adsorption

L. Borgnino [a,*], M.J. Avena [b], C.P. De Pauli [a]

[a] INFIQC, Departamento de Fisicoquímica, Facultad de Ciencias Químicas, Universidad Nacional de Córdoba, Ciudad Universitaria, 5000, Córdoba, Argentina
[b] INQUISUR, Departamento de Química, Universidad Nacional del Sur. Av. Alem 1253, 8000, Bahía Blanca, Argentina

ARTICLE INFO

Article history:
Received 19 November 2008
Received in revised form 13 March 2009
Accepted 21 March 2009
Available online 28 March 2009

Keywords:
Fe(III)-montmorillonite
Fe (hydr)oxide coating
Ferrihydrite
Phosphate adsorption

ABSTRACT

Two Fe(III)-modified montmorillonites were synthesized by mixing Fe(III) nitrate solutions with montmorillonite at pH 3.5 followed by an increase in pH up to 9. The synthesis procedure was analyzed by solubility calculations and Fe(III) speciation in aqueous solutions, and the resulting solids were characterized by X-ray diffraction, specific surface area, Mössbauer spectroscopy, electrophoretic mobilities (EM) and phosphate adsorption. At low pH, iron concentration in solution during the synthesis is controlled by adsorption/intercalation reactions, whereas at high pH the concentration is controlled by the solubility of ferrihydrite. When the initial Fe(III) content is relatively low the synthesized solid contains mainly interlayer/sorbed Fe(III). When the initial Fe(III) content is relatively high the synthesized solid contains also some iron (hydr)oxide phases, mainly ferrihydrite. These Fe(III) phases are in close contact with montmorillonite, either coating the montmorillonite surface or aggregated with montmorillonite particles. The presence of Fe(III) species increases significantly the specific surface area and phosphate adsorption capacity, but changes only slightly the EM of the solid.

1. Introduction

Many reactions in natural aquatic environments result in a multi-component solid with surface characteristics different from the original pure phases [1]. As an example, mineral weathering leads to the leaching of solutes, which can interact again with minerals to produce surface coatings (e.g., Fe (hydr)oxides coating phyllosilicates) that are often observed in soils and sediments [2–4]. Many studies have shown the importance of these surfaces coating, and there is considerable evidence that they play a dominant role in determining the transport, fate, biogeochemistry, bioavailability and toxicity of nutrients, pollutants and trace metals in natural waters [5]. Phyllosilicates, organic matter and Fe/Mn/Al (hydr)oxides are the major solid components in soil and sediments. Manganese oxides, iron oxides and organic materials are recognized as the three most important components in surface coatings, affecting the adsorption of nutrients, metal and other pollutants on solid minerals phase [6].

Phosphorus is an essential nutrient in aquatic environments. The geochemical behaviors of phosphate have been the subject of numerous studies in various disciplines [7,8]. An excessive concentration of this nutrient in water is the cause of eutrophication in lakes and reservoirs, and is a threat to ecological health. Adsorption of phosphate onto particulate matter is an important process that affects significantly the mobility and bioavailability of phosphorus in natural environments. Laboratory experiments have demonstrated that iron oxides are strong sorbents for phosphate, and they appear to dominate the solution chemistry in natural waters [9–11]. Goethite (α-FeOOH) is one of the most common crystalline iron oxyhydroxides in natural environments. Consequently, the adsorption behavior of phosphate on goethite, and its competitive interaction with other elements (e.g., organic matter, arsenate) have been studied in detail [10,12–18]. However, the adsorption behavior of phosphate may be different from that inferred directly by working with goethite, since phosphate is not only adsorbed on pure Fe (hydr)oxides, but also in Fe (hydr)oxides coatings. Very few studies have been carried out on the adsorption behavior of phosphate on Fe (hydr)oxides coating phyllosilicates [19] or aluminosilicates [20].

The modification of expandable phyllosilicates with Fe(III) species has been studied over the last decade in order to obtain the so-called Fe(III)-exchanged or Fe(III)-pillared materials. These materials have shown important potential application as catalysts in organic synthesis and in oxidation-reduction reactions [21–23]. Little is known about the adsorption properties on these systems [24,25], and particularly scarce is the information about phosphate adsorption on phyllosilicates and Fe(III)-modified clays [26].

In this study two Fe(III)-modified montmorillonites were synthesized and studied. The aim is to characterize the synthesized

* Corresponding author. Fax: +54 351 4334188.
E-mail addresses: borgnino@mail.fcq.unc.edu.ar (L. Borgnino), mavena@uns.edu.ar (M.J. Avena), depauli@mail.fcq.unc.edu.ar (C.P. De Pauli).

0927-7757/$ – see front matter © 2009 Elsevier B.V. All rights reserved.
doi:10.1016/j.colsurfa.2009.03.037

samples by X-ray diffraction (XRD), specific surface area (SSA) measurements, Mössbauer spectroscopy and electrophoretic mobilities (EM), and to compare their phosphate adsorption capacity with that of a non-modified montmorillonite.

2. Materials and methods

2.1. Preparation of Na-montmorillonite

The montmorillonite used in this study was obtained from Cerro Banderita (province of Neuquén, Argentina). Peinemann et al. [27] reported the chemical composition, structure, and some spectroscopic properties of this clay. Particles with diameter <2 μm were obtained by sedimentation and saturated with Na^+ by keeping the clay suspension in 1 M NaCl for 24 h. After that, the sample was washed with purified water to remove the excess of Na^+. Finally, the suspension was centrifuged, the supernatant removed and the solid was dried at 60 °C. This sodium-exchanged clay will be called Na-M. Its cation exchange capacity is 91.7 meq./100 g [27].

2.2. Preparation of Fe(III)-modified montmorillonites

Two different Fe(III)-modified montmorillonites with different iron contents were prepared. For the synthesis of the first sample, a weighed amount of solid $Fe(NO_3)_3{\cdot}9H_2O$ was dissolved in water to obtain a 0.01 M Fe(III) solution and its pH was adjusted to 3.5 with NaOH. Then, 550 mL of this clear fresh solution were mixed with 250 mL of a 2.2% Na-M dispersion in water, whose pH was adjusted to 3.5 before the mixing. After 2 h of vigorous magnetic stirring at this pH, a NaOH solution was added drop wise until pH 9. During this last procedure, several aliquots were withdrawn at different pH and centrifuged at 8690 g in order to quantify the concentration of Fe(III) remaining in the supernatant. Once at pH 9, the dispersion was stirred for other 3 h and then the solid was washed with water and dried at 60 °C for 3 days. This sample will be called Fe-M(1).

The same procedure was applied for the synthesis of the second Fe(III)-modified montmorillonite, except that 1100 mL of the 0.01 M Fe(III) solution were used. This sample will be called Fe-M(2).

All the solutions were prepared from analytical reagent grade chemicals and purified water (Milli-Q system). Both syntheses were carried out under nitrogen bubbling in order to avoid carbonate contamination.

2.3. Characterization methods

Fe and Na contents of the studied samples were measured by digesting 0.4 g of solid with hot (200 °C and 75 bar) mixtures of concentrated HNO_3 and H_2O_2 using an Anton Paar Microwave 3000 instrument. This method leaves a minute white and solid silicate residue, but can extract all the added iron and most of the structural iron. Fe and Na quantification in the resulting solution was performed using an AA-3000 PerkinElmer flame atomic absorption spectrometer.

The specific surface area was measured by the single-point N_2 adsorption method with a STROHLEIN area meter II instrument. An appropriate amount of dry solid (previously outgassed at 105 °C) was placed in contact with N_2 and the system was cooled to 77 K to produce and quantify the gas adsorption. The SSA of the sample was calculated from the adsorbed amount, taking into account that each N_2 molecule covers an area of 16 $Å^2$.

Powder X-ray diffraction patterns were recorded on a Philips XïPert PRO X-ray diffractometer, using Cu K_α radiation (30 kV–15 mA). XRD data was obtained in the 2θ range from 4° to 70° (step size: 0.01; 6 seg/step). For a better visualization of the 0 0 1 reflection, XRD pattern were also obtained from 4° to 15° (step size: 0.01; 4 seg/step). The reflections assignments were done using the software XïPert HighScore, installed on the X-ray diffractometer.

Mössbauer spectroscopy studies were carried out a room temperature using a $^{57}Co/Rh$ source in a constant-acceleration transmission spectrometer, which was calibrated using a standard α-Fe foil. All spectra were least squares fitted with Lorentzian lines shapes.

Electrophoretic mobilities measurements were carried out using a Rank Brothers Mark II electrophoresis apparatus equipped with a cylindrical cell. Approximately 200 mL, of a dilute montmorillonite suspension were prepared by dispersing a clay sample in 0.01 M NaCl. The pH of the suspension was raised to approximately 9 with NaOH and an EM measurement was carried out. After that, the pH was slightly decreased with HCl and a new EM measurement performed. This procedure was continued until the pH was around 3.5. To check reversibility, EM measurements were also performed by increasing the pH from 3.5 to 9. Each reported data is the average of the reading of 20 individual particles. To study the effect of phosphate on the EM of the studied samples, measurements at different pH were carried out in a similar way to solids suspended in 0.01 M NaCl in the presence of 0.01 M phosphate

2.4. Adsorption studies

Phosphate adsorption isotherms were performed with the solid samples. Preliminary experiments carried out at pH 4.5, 7.0 and 9.0 showed that adsorption decreases as the pH increases. Thus, for comparative purposes and in order to have a relatively high adsorption with all the studied samples, pH 4.5 was selected as the pH for these experiments. The effect of pH, spectroscopy of adsorbed phosphate species and the mechanism involved on phosphate adsorption will be the topic of a forthcoming paper.

For each data point of the isotherm with Na-M, 1 g of solid was suspended in 40 mL of a 0.01 M NaCl solution and the pH of this mixture was adjusted to 4.5 by addition of a HCl solution. A well-known volume of a 0.01 M phosphate solution ($NaH_2PO_4{\cdot}H_2O$), prepared in 0.01 M NaCl and having also a pH 4.5, was then added to the suspension. Any change in pH after the mixing was readjusted by adding either HCl or NaOH solutions. After 24 h of equilibration, the pH was registered, the suspension was centrifuged, the supernatant analyzed for phosphate concentration and the adsorbed amount calculated. Several data points were obtained as described by using different volumes of the phosphate solution. In the case of isotherms with Fe-M(1) or Fe-M(2), the same procedure was followed except that 0.1 g of solid and 40 mL of the phosphate-0.01 M NaCl solution were used. Phosphate concentration was quantified following the method proposed by Murphy and Riley [28].

3. Results and discussion

The distribution of Fe(III) species as a function of pH for a 0.01 M Fe(III) aqueous solution is shown in Fig. 1a. Curves were calculated using the software MINEQL+ 3.01b [29] assuming no precipitation of solid phases and using equilibrium constants, *K*, of the reactions listed in Table 1. The values of *K* correspond to those already included in the software MINEQL+, and they coincide with the well-known data informed by Baes and Mesmer [30], except for the case of formation of aqueous $Fe(OH)_3$. Since a freshly prepared 0.01 M Fe(III) nitrate solution at pH 3.5 is completely clear and contains no solid particles, the distribution of species at this pH can be directly evaluated from Fig. 1a. At pH 3.5 the used 0.01 M Fe(III) solution is mainly an equimolar mix of $Fe(OH)^{2+}$ and $Fe(OH)_2{}^+$ monomers with small amounts of Fe^{3+}, $Fe_2(OH)_2{}^{4+}$ and $Fe_3(OH)_4{}^{5+}$ species. They are all positively charged species that may have significant affinity for the surface of montmorillonite. In fact, when this Fe(III)

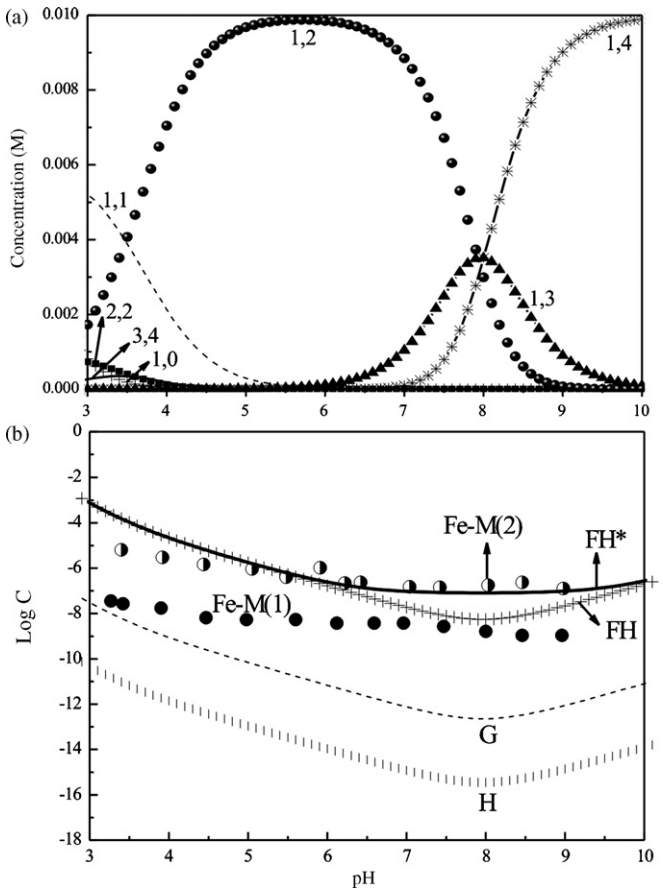

Fig. 1. (a) Distribution of Fe(III) species as a function of pH for a 0.01 M Fe(III) aqueous solution. Numbers in the figure refer to the following aqueous Fe(III) species: 1,0: Fe^{3+}; 1,1: $Fe(OH)^{2+}$; 1,2: $Fe(OH)_2^{+}$; 1,3: $Fe(OH)_3$; 1,4: $Fe(OH)_4^{-}$; 2,2: $Fe_2(OH)_2^{4+}$; 3,4: $Fe_3(OH)_4^{5+}$. (b) Dissolved Fe(III) concentration during the synthesis of Fe-M(1) and Fe-M(2) and comparison with the solubility curves of different Fe (hydr)oxides. Calculations were performed with data in Table 1. FH, ferrihydrite; FH*, ferrihydrite with data from Baes and Mesmer [30]; G, goethite; H, hematite.

solution is mixed with the montmorillonite suspension at pH 3.5, uptake of Fe(III) species took place and most of Fe(III) species were removed from the solution. This is shown in Fig. 1b where the total Fe(III) concentration that remained in the supernatants is plotted as a function of pH. At pH 3.5 the concentration of Fe(III) is 2×10^{-8} M for the case of the synthesis of Fe-M(1) and 6×10^{-6} M for that of Fe-M(2), values that are much lower than the initial ones. At higher pH, a decrease in iron concentration is observed indicating that the uptake of iron species becomes even more important as pH increases.

Table 1
Log K values of the different equilibria used for Fe(III) speciation. Values were obtained from the MINEQL+ software.

Aqueous species	Equilibrium	Log K
$Fe(OH)^{2+}$	$Fe^{3+} + H_2O \leftrightarrows Fe(OH)^{2+} + H^+$	−2.19
$Fe(OH)_2^{+}$	$Fe^{3+} + 2H_2O \leftrightarrows Fe(OH)_2^{+} + 2H^+$	−5.67
$Fe(OH)_3$	$Fe^{3+} + 3H_2O \leftrightarrows Fe(OH)_3 + 3H^+$	−13.6 (<−12)*
$Fe(OH)_4^{-}$	$Fe^{3+} + 4H_2O \leftrightarrows Fe(OH)_4^{-} + 4H^+$	−21.6
$Fe_2(OH)_2^{4+}$	$2Fe^{3+} + 2H_2O \leftrightarrows Fe_2(OH)_2^{4+} + 2H^+$	−2.95
$Fe_3(OH)_4^{5+}$	$3Fe^{3+} + 4H_2O \leftrightarrows Fe_3(OH)_4^{5+} + 4H^+$	−6.3
Solids		
α-FeOOH (goethite)	$Fe^{3+} + 2H_2O \leftrightarrows FeOOH(s) + 3H^+$	−0.5
α-Fe_2O_3 (hematite)	$2Fe^{3+} + 3H_2O \leftrightarrows Fe_2O_3(s) + 6\,H^+$	4.01
Freshly prepared Fe(III) hydroxide or ferrihydrite	$Fe^{3+} + 3H_2O \leftrightarrows Fe(OH)_3(s) + 3H^+$	−4.89

* Value within brackets was obtained from Baes and Mesmer [30].

For comparison, Fig. 1b also shows the solubility of different Fe(III) (hydr)oxides (ferrihydrite, goethite and hematite) as a function of pH. Since equilibrium data included in the MINEQL+ software differ in one case from those reported by Baes and Mesmer [30] (Table 1), for the case of ferrihydrite two solubility curves are shown, one using $\log K = -13.6$ for the formation of aqueous $Fe(OH)_3$ and the other one using $\log K = -12$. For goethite and hematite the value of $\log K = -13.6$ was used. Fe(III) concentrations in the supernatant during the synthesis of Fe-M(1) do not coincide with any of the solubility curves, indicating that the considered solid phases are not controlling the concentrations of Fe(III). The only exception may be for data between pH 7 and 9, where iron concentration approaches the solubility curves of ferrihydrite. Data suggest that in the case of the synthesis of Fe-M(1) iron concentration in solution is mainly controlled by reactions other than precipitation–dissolution reactions, probably sorption reactions such as adsorption at the external surfaces and/or exchange with sodium ions in the interlayer. Only at pH >7 some ferrihydrite might be formed. The case of Fe-M(2) is different. Iron concentrations do not coincide with solubility curves at pH <5, but between pH 5 and 9 there is a remarkable coincidence with one of the solubility curves of ferrihydrite. This suggests that sorption reactions are still controlling the iron concentrations at pH <5 but that ferrihydrite is formed at pH >5, and thus the solubility of this solid takes control of iron concentration. Formation of ferrihydrite in the presence of montmorillonite was also reported by Green-Pedersen and Pind [31], who used a synthesis method very similar to the present method, mixing montmorillonite and Fe(III) solutions at pH 2.5 and then slowly raising the pH up to 8.

Table 2 shows the Fe content, the Na content and the SSA of the studied samples. Fe content of Na-M is 27.6 mg/g, a value that is similar to the previously measured (30 mg/g) by Peinemann et al. [27] by fusion of the solid with sodium carbonate. The content is relatively low as compared to those of Fe-M(1) (77 mg/g) and Fe-M(2) (154 mg/g). The results are in agreement with Fe concentrations measured in supernatants at different pH, indicating that most of the initial iron is removed from solution during the synthesis of the samples, resulting in an iron content that increases in the order Na-M < Fe-M(1) < Fe-M(2). The increase in Fe content is corresponded with a decrease in Na content, showing that an important fraction of sodium is displaced by iron in the interlayer. The increase in Fe content also leads to an increase in the SSA of the solids, as measured by N_2 adsorption. Na-M has a relatively low SSA of 12 m^2/g, value that is rather normal for montmorillonite, and represents the external surface area of the clay, since nitrogen molecules cannot enter the interlayer spacing. Fe-M(1) and Fe-M(2) have larger SSA values. The results are in agreement with data reported by other authors. Manjanna [32], for example, showed that increasing the iron content of Fe(III)-montmorillonites increased the SSA of the samples, and suggested that this increase in the SSA is the result of the presence of associated Fe-oxide phases. Similarly, Nguyen-Thanh et al. [33] informed that a Fe-montmorillonite had a SSA of 63 m^2/g as compared to 33 m^2/g of a Na-montmorillonite, and attributed these changes to changes in the porosity of the samples because of the presence of iron oxide clusters on the outer surfaces of the clay particles. The results of Green-Pedersen and Pind [31] are also in line with these interpretations. They synthesized montmorillonite particles coated with ferrihydrite and attributed

Table 2
Na, Fe content and SSA of the studies solids.

Sample	Fe content (mg/g)	Na content (mg/g)	SSA (m^2/g)
Na-M	27.6	16	12
Fe-M(1)	77	4.7	52
Fe-M(2)	154	1.3	123

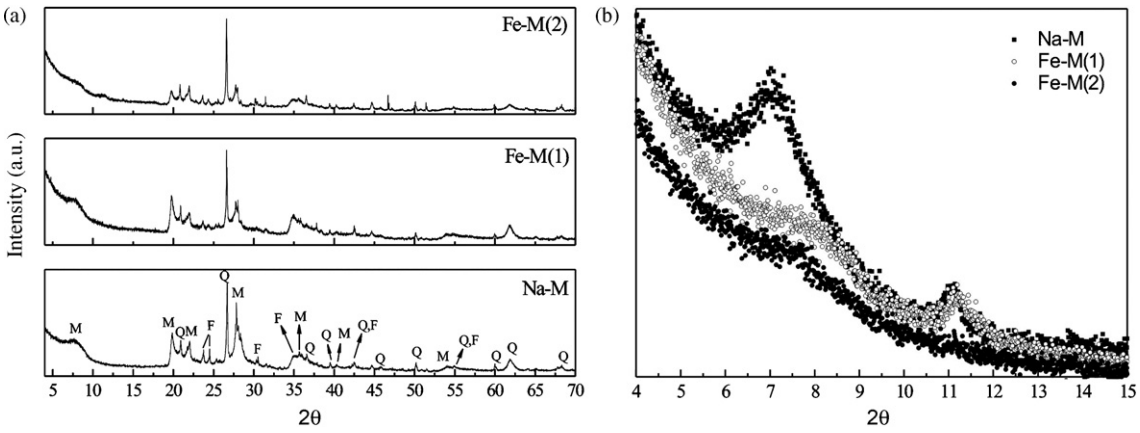

Fig. 2. XRD patterns of (a) Na-M, (b) Fe-M(1) and (c) Fe-M(2). Reflections assignments are as follows: M, montmorillonite; Q, quartz; F, feldspar.

the increase of the SSA to the presence of ferrihydrite, even though the SSA of the Fe-montmorillonite was much higher than the area calculated based on a simple mixing model applied to the pure phases (montmorillonite and ferrihydrite). A different explanation was given by Yuan et al. [34]. They proposed a delaminated structure for Fe(III)-montmorillonites where Fe(III) polyoxocations and montmorillonite are combined to give a "house of cards" structure with mesopores. The situation of Fe-M(1) and Fe-M(2) seems to represent one of these cases or a mix of them. The presence of some ferrihydrite, which usually has a relatively large SSA of around 300 m^2/g [31], or other associated Fe-oxide phases would increase the SSA of the solids. In addition, the presence of adsorbed iron species, ferrihydrite or other phases associated to montmorillonite would modify the aggregation properties of the clay layers leading to a solid with higher porosity and larger SSA.

The XRD patterns of the three studied samples are shown in Fig. 2a. The pattern of Na-M is typical of a sodium-exchanged montmorillonite [35] with quartz [31] and perhaps some feldspars impurities. It shows the 0 0 1 reflection at 7.01°2θ, corresponding to a basal spacing, d_{001}, of 12.6 Å, which is normal for a sodium montmorillonite [36]. The XRD pattern of Fe-M(1) is very similar to that of Na-M. The 0 0 1 reflection is less intense and appears at a slightly higher angle, around 7.72°2θ corresponding to a lower basal space, d_{001} = 11.45 Å (Fig. 2b). Changes in the basal spacing depend on the charge, size and hydration behavior of the ion or molecule that is located in the interlayer and on interactions between it and the phyllosilicate layers. The ionic radius of Fe^{3+} and Na^+ are respectively 0.65 Å and 1.02 Å, whereas in their hydrated form the Fe–O bond length is 2.0 Å (for the case of $[Fe(OH_2)_6]^{3+}$ species) and the Na–O length is 2.4 Å (for the case of $[Na(OH_2)_6]^+$ species) [37]. The smaller size of iron can in principle explain the decrease in the basal spacing. Decrease in d_{001} by addition of Fe(III) has been also observed for example by Chen et al. [38], who attributed this effect to strong attractive forces between iron and the silicate sheets of montmorillonite. Other authors, on the contrary, have observed a slight increase in d_{001} probably due to the presence of polymeric species of iron within the interlayer [22,35]. Even delaminated clays that lost their 0 0 1 diffraction peak could be synthesized after relatively long reaction times (e.g., over 12 h) and high temperatures [38,39]. Similarly, Nguyen-Thanh et al. [33] have found no well-defined 0 0 1 diffraction peaks for Fe-montmorillonites, attributing these effects to adsorption of iron oxocations of different sizes or to delamination. The XRD pattern of Fe-M(1) is in agreement with the differences in size of iron and sodium, suggesting that at least part of the added Fe(III) is present in the interlayer space. The fact that sodium content in Fe-M(1) is lower than in Na-M gives additional and independent evidence for this intercalation. If some ferrihydrite is formed as an associated phase, it is not detected in the diffraction pattern since the typical broad reflections of ferrihydrite at 35°2θ and 62°2θ [40] do not appear.

The XRD pattern of Fe-M(2) is very similar to that of Fe-M(1), and the 0 0 1 reflection is also around 7.75°2θ (d_{001} = 11.39 Å). Thus, part of the Fe(III) seems to be present in the interlayer space. Even though solubility data strongly suggest that ferrihydrite is formed in this sample (Fig. 1b), no characteristics reflections peaks of this phase appear. It is possible that ferrihydrite is forming thin coatings or very small clusters or particles that cannot be detected by XRD. Indeed, Yuan et al. [41] have found by HRTEM that Fe(III)-treated montmorillonites contained iron oxide co-aggregates/nanoparticles with a mean size of 6 nm.

The Mössbauer spectra of the samples are shown in Fig. 3. The parameters obtained from the least squares analysis together with the assignment of different components are given in Table 3. There is one doublet for Na-M and two doublets for Fe-M(1) and Fe-M(2). Structural (lattice) iron is the responsible of the spectrum of Na-M giving IS 0.35 mm/s and QS 0.46 mm/s, being consistent with Fe(III) in octahedral positions [42]. This structural iron is also detected in Fe-M(1) together with another form of iron with parameters IS 0.35 mm/s and QS 0.82. According to van der Zee et al. [43], these values for IS and QS indicate iron octahedrally coordinated with O and OH groups, such as Fe in oxides, phyllosilicates, and other Fe(III) bearing silicates. This seems to be iron in close contact with silicates and could be assigned to either Fe(III) species within the interlayer spaces or Fe(III) species adsorbed at the outer surfaces, in agreement with the evidences found from solubility curves (Fig. 1b). Since it is not possible to differentiate between these two types of Fe(III) species, they will be grouped together and called interlayer/sorbed Fe(III). In the case of Fe-M(2), structural iron is not detected perhaps because its content is rather low as compared to the iron incorporated during the synthesis of the sample. The spectrum shows the doublet corresponding to interlayer/sorbed Fe(III) species and another doublet with IS 0.35 mm/s and 0.62 mm/s,

Table 3
Mössbauer parameters of samples determined from spectra collected at room temperature.

Sample	IS (mm/s)	QS (mm/s)	Abundance (%)	Assignment
Na-M	0.35	0.46	100	Fe(III) in clay
Fe-M(1)	0.35	0.46	37	Fe(III) in clay
	0.35	0.82	63	Interlayer/sorbed Fe(III)
Fe-M(2)	0.35	0.82	54	Interlayer/sorbed Fe(III)
	0.35	0.62	46	Ferrihydrite

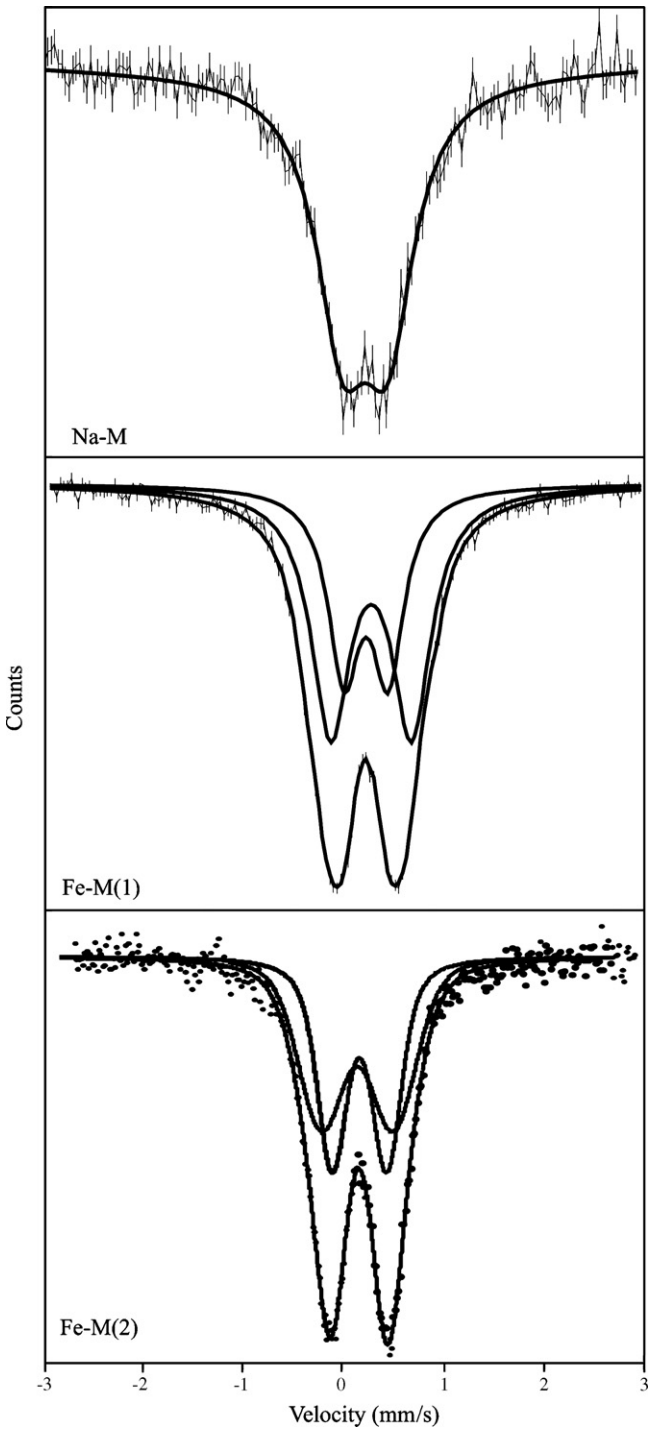

Fig. 3. Mössbauer spectra at room temperature of the studied solids.

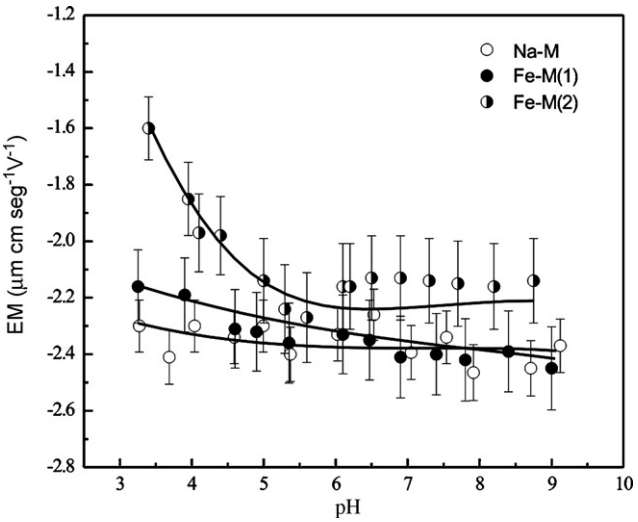

Fig. 4. Electrophoretic mobilities of the three studied solids in 0.01 M NaCl.

which is characteristic of ferrihydrite [44–46]. Mössbauer spectra agree with solubility and allow to confirm that added iron in Fe-M(1) becomes mainly interlayer/sorbed Fe(III) whereas in Fe-M(2) becomes a mix of interlayer/sorbed Fe(III) and ferrihydrite. Since 46% of the added iron is present as ferrihydrite ($5Fe_2O_3{\cdot}9H_2O$) in Fe-M(2) (Table 3), this sample contains around 0.13 g of ferrihydrite per gram of montmorillonite.

Fig. 4 shows the EM vs. pH curves of three studied samples in 0.01 M NaCl solutions. Na-M and Fe-M(1) show very similar behavior, with EM always negative and almost unchanged between pH 3 and 9. The EM of Fe-M(2) is also negative in the investigated pH range, although it is less negative than that of the other samples, and some pH dependency is observed at pH <5.5. It must be remarked that all the particles observed when performing EM measurements to Fe-M(1) and Fe-M(2) had negative EM. This indicates that ferrihydrite and the other iron (hydr)oxide phases that could be present in the samples are in close contact with montmorillonite particles, either forming surface clusters or coating the surface of montmorillonite. Otherwise, individual particles with positive EM should have been observed in these experiments at low pH, where iron (hydr)oxides have positive EM [31,46–48].

The behavior of Na-M is well-known [49–51], and is the result of the presence of structural negative charges within the clay lattice. The positive charge that can be generated at the broken edges of the clay layers at low pH is not enough to produce significant modification in the EM because this charge is much lower than the structural charge [52]. The presence of interlayer/sorbed Fe(III) species does not modify the electrophoretic behavior of the solid, as can be deduced from the EM data of Fe-M(1). Since 1 mmol of iron was added per gram of montmorillonite in the synthesis of this sample, the electrical charges provided by iron would be 300, 200 or 100 meq./100 g of montmorillonite if interlayer/sorbed Fe(III) is present as Fe^{3+}, $Fe(OH)^{2+}$ or $Fe(OH)_2^{+}$ respectively. In all these cases iron would have been able to completely neutralize the structural charge of montmorillonite (91.7 meq./100 g) and even to produce charge reversal. The fact that no changes in the EM are produced indicates that interlayer/sorbed Fe(III) is present either at the surface or within the interlayer space of montmorillonite as neutral or near neutral species, which could be formed after raising the pH to 9 in the synthesis.

Fe-M(2) has negative EM in the studied range of pH, and shows a decrease in this negative EM at pH lower than 5. This decrease is presumably due to the presence of ferrihydrite and other iron (hydr)oxide phases, which are known to be positively charged at low pH. Simple calculations can be performed to estimate the charge provided by ferrihydrite or other iron (hydroxides) in Fe-M(2) assuming that this sample is a mix of ferrihydrite and montmorillonite. Iron (hydr)oxides have a positive charge of around 0.2 C/m^2 at pH 4 and 0.01 M electrolyte concentration [48]. If a SSA of 300 m^2/g is assumed for ferrihydrite [46,47] this results in a net positive charge of 62 meq./100 g of ferrihydrite. Therefore, in 1.3 g of a ferrihydrite–montmorillonite mixture containing 0.13 g of ferrihydrite and 1 g of pure montmorillonite, ferrihydrite will provide 0.08 meq. of positive charges and montmorillonite 0.917 meq. of negative charges. This could be enough to decrease somewhat the

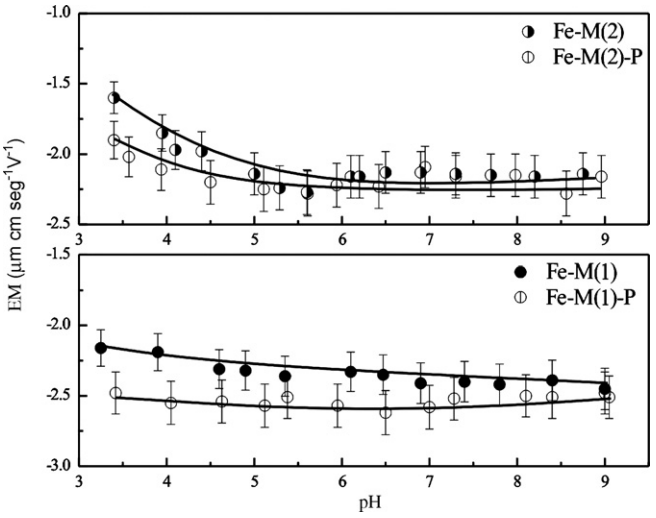

Fig. 5. Electrophoretic mobilities of Fe-M(1) and Fe-M(2) in absence and presence of 0.01 M phosphate in 0.01 M NaCl solutions.

EM at low pH, but not to produce charge reversal, in agreement with electrophoretic data.

Fig. 5 shows the EM vs. pH curves of Fe-M(1) and Fe-M(2) in absence and presence of phosphate. Although the changes are not very large, in both cases phosphate increases the negative EM, suggesting phosphate adsorption.

Fig. 6 shows phosphate adsorption isotherms at pH 4.5 for the three samples. Lines in the figure were drawn only to serve as guides to the eyes. The adsorption per unit area increases in the order Na-M < Fe-M(1) < Fe-M(2), in line with the increase in the iron content. If adsorption per unit mass (instead of adsorption per unit area as shown in the figure) is considered, the differences are even more important because of the different SSA of the samples. For example, adsorption values at equilibrium phosphate concentrations of around 10^{-3} M are 6.0×10^{-6}, 9.4×10^{-5} and 3.3×10^{-4} mol/g for Na-M, Fe-M(1) and Fe-M(2) respectively, indicating that the phosphate adsorption capacities of Fe-M(1) and Fe-M(2) are 16 and 55 times larger than that of Na-M. In addition, and although data are not shown here, it may be mentioned that Fe-M(1) and Fe-M(2) samples are also good phosphate adsorbents at higher pH. For the case of Fe-M(1), for example, adsorption at 10^{-3} M phosphate concentration was 9.3×10^{-5}, 7.5×10^{-5} and 4.2×10^{-5} mol/g for pH 4.5, 7.0 and 9.0 respectively. On the contrary, no adsorption was detected for Na-M at pH 7.0 and 9.0.

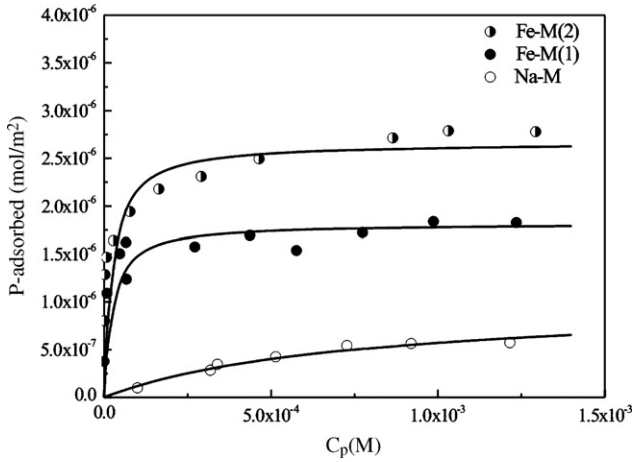

Fig. 6. Phosphate adsorption on Na-M, Fe-M(1) and Fe-M(2) at pH 4.5 in 0.01 M NaCl.

It is well known that phyllosilicate clays such as montmorillonite have a very low affinity for phosphate. The low affinity is mainly because the 0 0 1 basal surface is the main surface exposed to the aqueous solution. The presence of the rather unreactive siloxane group and negative structural charges impedes phosphate adsorption at this surface. Only clay edges, which can develop positive charges at low pH and rather reactive surface groups [52,53], could adsorb phosphate electrostatically or by a ligand exchange process. However, since the edge surface represents only a small fraction of the total clay surface area, adsorption at clay edges would not contribute significantly to phosphate adsorption, giving relatively low adsorption values as shown in Fig. 6. Moreover, at intermediate or high pH, where clay edges are negatively charged, the adsorption will be lower or even negligible as seen with Na-M. On the contrary to what happens with montmorillonite, ferrihydrite, goethite and other Fe(III) (hydr)oxides are very good phosphate adsorbents [47,48]. There are also reports indicating that clays coated with Fe (hydr)oxides are better phosphate adsorbent than pure montmorillonite [25,54]. Thus, phosphate adsorption on Fe-M(1) and Fe-M(2) should be mainly due to the presence of these solid phases and to the presence of interlayer/sorbed Fe(III) species. The adsorption of phosphate by iron (hydr)oxide phases can also explain the change in EM towards more negative values in phosphate solutions, and the decrease in the adsorption as the pH increases, which is a well know property of iron (hydr)oxides [47,48].

According to Arai and Sparks [47], phosphate adsorption on pure ferrihydrite at pH 4.5 is around 1.6×10^{-6} mol/m^2. This value is lower than those of Fe-M(1) (1.8×10^{-6} mol/m^2) and Fe-M(2) (2.7×10^{-6} mol/m^2), indicating that the synthesized Fe(III)-modified montmorillonites have surface characteristics different from a simple mixture of montmorillonite and ferrihydrite. In the case of Fe-M(1), the high adsorption capacity with respect to ferrihydrite has to be attributed to the presence of interlayer/sorbed Fe(III), which is the main iron component of this sample. Sorbed species at the outer surfaces are surely more active than interlayer species because it should be easier for phosphate to adsorb at the outer surface than entering the interlayer space. In the case of Fe-M(2), both interlayer/sorbed Fe(III) and ferrihydrite must contribute to the adsorption. It seems that these Fe(III) species are well disperse and active due to the presence of the montmorillonite surface.

4. Conclusions

The mix of 0.01 M Fe(III) solutions and montmorillonite at pH 3.5 followed by an increase in pH up to pH 9 results in two types of synthetic Fe(III)-modified montmorillonites. When the amount of Fe(III) solution is relatively low, intercalation and adsorption of iron takes place leading to a montmorillonite sample that contains mainly interlayer/sorbed Fe(III). When the amount of Fe(III) solution is relatively high, iron (hydr)oxide phases such as ferrihydrite are formed besides interlayer/sorbed Fe(III). In both cases, iron species and phases are in close contact with montmorillonite, since no individual positively charged particles could be detected by electrophoresis. The synthesized samples are relatively good phosphate adsorbent. Phosphate adsorption is significantly higher on these samples than on pure montmorillonite. On a per area basis, phosphate adsorption is also higher than on pure ferrihydrite. Both, interlayer/sorbed Fe(III) and ferrihydrite, contribute significantly to the adsorption.

Acknowledgments

The authors thank CONICET and SECyT for financial support. L.B thanks CONICET for the fellowship granted. Thanks are also due to

Dr. Juan Pablo Gaviría for the assistance in the performance and interpretation of Mössbauer spectroscopy and Mr. Oscar Sandín (CNEA-Córdoba) for SSA measurements.

References

[1] P.R. Anderson, M.M. Benjamín, Surface and bulk characteristic of binary oxide suspensions, Environ. Sci. Technol. 24 (1990) 692–698.
[2] Y. Xu, L. Axe, Synthesis and characterization of iron oxide-coated silica and its effects on metal adsorption, J. Colloid Interface Sci. 282 (2005) 11–19.
[3] L. Borgnino, C. Oroná, M. Avena, A. Maine, A. Rodríguez, C.P. De Pauli, Phosphate concentration an association as revealed by sequential extraction and microprobe analysis: the case of sediments from two Argentinean Reservoirs, Water Resour. Res. 42 (2006) W01414, doi:10 1029/2005WR004031.
[4] T. Hou, R. Xu, D. Tiwari, A. Zhao, Interaction between electrical double layers of soil colloids and Fe/Al oxides in suspension, J. Colloid Interface Sci. 310 (2007) 670–674.
[5] W.J. Weber, P.M. Mc Ginleys, L.E. Katz, Sorption phenomena in subsurface systems: concepts, models and effects on contaminant fate and transport, Water Res. 25 (1991) 499–528.
[6] D. Perret, J. Gaillard, J. Dominik, O. Atteia, The diversity of natural hydrous iron oxides, Environ. Sci. Technol. 34 (2002) 3540–3546.
[7] L. Borgnino, M. Avena, C.P. De Pauli, Surface properties of sediments from two Argentinean reservoirs and the rate of phosphate release, Water Res. 40 (2006) 2659–2666.
[8] B.M. Spears, L. Carvalho, R. Perkins, A. Kirika, D.M. Paterson, Spatial and historical variation in sediment phosphorous fraction and mobility in a large shallow lake, Water Res. 40 (2006) 383–391.
[9] M.L. Pierce, C.B. Moore, Adsorption of arsenite and arsenate on amorphous iron hydroxide, Water Res. 16 (1982) 1247–1253.
[10] N. Nilsson, P. Persson, L. Lovgren, S. Sjoberg, Competitive surface complexation of o-phtalate and phosphate on goethite (α-FeOOH) particles, Geochim. Cosmochim. Acta 60 (1996) 4385–4395.
[11] Y. Gao, A. Mucci, Acid base reactions, phosphate and arsenate complexation, and their competitive adsorption at the surface of goethite in 0.7 M NaCl solution, Geochim. Cosmochim. Acta 65 (2001) 2361–2378.
[12] L. Sigg, W. Stumm, The interaction of anions and weak acids with the hydrous goethite surface, Colloid Surf. 2 (1981) 101–117.
[13] S. Goldberg, Chemical modeling of arsenate adsorption on aluminum and iron oxide minerals, Soil Sci. Soc. Am. J. 50 (1986) 1154–1157.
[14] J.S. Geelhoed, T. Hiemstra, W.H. van, Riemsdijk, Phosphate and sulfate adsorption on goethite: single anion and competitive adsorption, Geochim. Cosmochim. Acta 61 (1997) 2389–2396.
[15] R.P.J.J. Rietra, T. Hiemstra, W.H. van, Riemsdijk, Sulfate adsorption on goethite, J. Colloid Interface Sci. 218 (1999) 511–521.
[16] R.P.J.J. Rietra, T. Hiemstra, W.H. van, Riemsdijk, Interaction between calcium and phosphate adsorption on goethite, Environ. Sci. Technol. 35 (2001) 3369–3374.
[17] H. Zhao, R. Stanforth, Competitive adsorption of phosphate and arsenate on goethite, Environ. Sci. Technol 35 (2001) 4753–4757.
[18] J. Antelo, F. Arce, M.J. Avena, S. Fiol, R. López, F. Macías, Adsorption of a soil humic acid at the surface of goethite and its competitive interaction with phosphate, Geoderma 138 (2007) 12–19.
[19] J. Zhuang, G.-R. Yu, Effects of surface coating on electrochemical properties and contaminant sorption of clay minerals, Chemosphere 49 (2002) 619–628.
[20] A.A. Jara, S. Goldberg, M.L. Mora, Studies of the surface charge of amorphous aluminosilicates using surface complexation models, J. Colloid Interface Sci. 292 (2005) 160–170.
[21] A. Cornélis, P. Laszlo, Molding clays into efficient catalysts, Synlett (1993) 155–161.
[22] J.P. Chen, M.C. Hausladen, R.T. Yang, Delaminated Fe_2O_3-pillared clay: its preparation, characterization, and activities for selective catalytic reduction of NO by NH_3, J. Catal. 151 (1995) 135–146.
[23] A. Nait Ajjou, H. Dramé, C. Detellier, H. Alper, Cation-exchanged montmorillonite catalyzed hydration of styrene derivatives, J. Mol. Catal. A: Chem. 126 (1997) 55–60.
[24] V. Lenoble, O. Bouras, V. Deluchat, B. Serpaud, J.C. Bollinger, Arsenic adsorption onto pillared clays and iron oxides, J. Colloid Interface Sci. 3255 (2002) 52–58.
[25] T. Grygar, D. Hradil, P. Bezdička, B. Doušova, L. Čapek, O. Schneeweiss, Fe (III) modified montmorillonite and bentonites: synthesis, chemical and UV spectral characterization, arsenic sorption, and catalysis of oxidative dehydrogenation of propane, Clays Clay Miner. 55 (2007) 165–176.
[26] B.B. Yosef, U. Kafkari, R. Rosenberg, G. Sposito, Phosphorus adsorption by kaolinite and montmorillonite. I. Effect of time, ionic strength and pH, Soil Sci. Soc. Am. J. 52 (1988) 1580–1585.
[27] N. Peinemann, E.A. Ferreiro, A.K. Helmy, Estudio mineralógico de una montmorillonita de Cerro Bandera (Provincia de Neuquén, República Argentina, Revista de la Asociación Geológica Argentina 27 (1972) 399–410.
[28] J. Murphy, J.P. Riley, A modified single solution method for determination of phosphate in natural waters, Anal. Chem. 27 (1962) 31–36.
[29] J. Westall, J.L. Zachary, F.M.M. Morel, A computer program for the calculation of chemical equilibrium composition of aqueous systems, Massachusetts Institute of Technology, Cambridge, M.A., 1976.
[30] C.F. Baes, R.E. Mesmer, The Hydrolysis of Cations, Wiley, New York, 1976.
[31] H. Green-Pedersen, N. Pind, Preparation, characterization, and sorption properties for Ni(II) of iron oxyhydroxide–montmorillonite, Colloids Surf. A: Physicochem. Eng. Aspects 168 (2000) 133–145.
[32] J. Manjanna, Preparation of Fe(III)-montmorillonite by reduction of Fe(III)-montmorillonite with ascorbic acid, App. Clay Sci. 42 (2008) 32–38.
[33] D. Nguyen-Thanh, K. Block, T.J. Bandosz, Adsorption of hydrogen sulfide on montmorillonites modified with iron, Chemosphere 59 (2005) 343–353.
[34] P. Yuan, H. He, F. Bergaya, D. Wu, Q. Zhou, J. Zhu, Synthesis and characterization of delaminated iron-pillared clay with meso-microporous structure, Microporous Mesoporous Mater. 88 (2006) 8–15.
[35] H. Dramé, Cation exchange and pillaring of smectites by aqueous Fe nitrate solution, Clays Clay Miner. 53 (2005) 335–347.
[36] R.E. Grim, International Series in Earth and Planetary Sciences, Mc. Graw-Hill, New York, 1953.
[37] D. Richens, The Chemistry of Aqua Ions, John Wiley & Sons, Chichester, 1997.
[38] G. Chen, B. Han, H. Yan, Interaction of cationic surfactants with iron and sodium montmorillonite suspensions, J. Colloid Interface Sci. 201 (1998) 158–163.
[39] M.N. Timofeeva, S.Ts. Khankhasaeva, S.V. Badmaeva, A.L. Chuvilin, E.B. Burgina, A.B. Ayupov, V.N. Panchenko, A.V. Kulikova, Synthesis, characterization and catalytic application for wet oxidation of phenol of iron-containing clays, Appl. Catal. B: Environ. 59 (2005) 243–248.
[40] R.M. Cornell, U. Schwertmann, The Iron Oxides: Structure, Properties, Reactions, Occurrence and Uses, WCH, Weinheim, New York, 2004.
[41] P. Yuan, F. Annabi-Bergaya, Q. Tao, M. Fan, Z. Liu, J. Zhu, H. He, T. Chen, A combined study by XRD, FTIR, TG and HRTEM on the structure of delaminated Fe-intercalated/pillared clay, J. Colloid Interface Sci. 324 (2008) 142–149.
[42] A. Kulshreshtha, A. Tripathi, T.N. Agarwal, K.R. Patel, M.S. Sisodia, R.P. Tripathi, ^{57}Fe Mössbauer spectroscopy study or organic rich sediments (source rock) from test well CPT-1 and MDP-1 located in Eastern Krisna–Godavari basin, India, Fuel 83 (2004) 1333–1339.
[43] C. van der Zee, C.P. Slomp, D.G. Rancourt, G.J. de Lange, W. van, Raamphost, A Mössbauer spectroscopic study of the iron redox transition in eastern Mediterranean sediments, Geochim. Cosmochim. Acta 69 (2005) 441–452.
[44] M. Žic, M. Ristić, S. Musić, Fe Mössbauer, FT-IR and SEM investigation of the formation of hematite and goethite at high pH values, J. Mol. Struct. 834 (2007) 141–149.
[45] H. Liu, P. Li, M. Zhu, Y. Wei, Y. Sun, Fe(II) induced transformation from ferrihydrite to lepidocrocite and goethite, J. Solid State Chem. 180 (2007) 2121–2128.
[46] C. Mikutta, R. Mikutta, S. Bonneville, F. Wagner, A. Voegelin, I. Cristl, R. Kretzschmar, Synthetic coprecipitates of exopolysaccharides and ferrihydrite. Part I. Characterization, Geochim. Cosmochim. Acta 72 (2008) 1111–1127.
[47] Y. Arai, D. Sparks, ATR-FTIR spectroscopy investigation on phosphate adsorption mechanism at the ferrihydrite-water interface, J. Colloid Interface Sci. 241 (2001) 241–326.
[48] J. Antelo, M. Avena, S. Fiol, R. López, F. Arce, Effect of phosphate and ionic strength on the adsorption of phosphate and arsenate at the goethite-water interface, J. Colloid Interface Sci. 285 (2005) 476–486.
[49] S.E. Miller, P.F. Low, Characterization of the electrical double layer of montmorillonite, Langmuir 6 (1990) 572–578.
[50] M.J. Avena, C.P. De Pauli, Proton adsorption and electro-kinetics of an Argentinean montmorillonite, J. Colloid Interface Sci. 202 (1998) 195–204.
[51] F. Thomas, L.J. Michot, D. Vantelon, E. Montargès, B. Prélot, M. Cruchaudet, J.F. Delon, layer charge and electrophoretic mobility of smectites, Colloids Surf. A: Physicochem. Eng. Aspects 159 (1999) 351–358.
[52] M.J. Avena, Acid-base behavior of clay surfaces in aqueous media, in: P. Somasundaran, Dekker Marcel (Eds.), Encyclopedia of Surface and Colloid Science, New York, 2006, pp. 17–46.
[53] E.A. Ferreiro, S.G. Bussetti, A.K. Helmy, Effect of montmorillonite on phosphate sorption by hydrous Al-oxides, Geoderma 55 (1992) 111–118.
[54] J.B. Harsh, H.E. Doner, The nature and stability of aluminum hydroxide precipitated on Wyoming montmorillonite, Geoderma 36 (1985) 45–56.